## Modeling the April 1997 flare of Mkn 501

A. Mücke and R.J. Protheroe

The University of Adelaide

Dept. of Physics & Mathematical Physics

Adelaide, SA 5005, Australia

Abstract. The April 1997 giant flare of Mkn 501 is modelled by a stationary Synchrotron-Proton-Blazar model. Our derived model parameters are consistent with X-ray-to-TeV-data in the flare state and diffusive shock acceleration of  $e^-$  and p in a Kolmogorov/Kraichnan turbulence sprectrum. While the emerging pair-synchrotron cascade spectra initiated by photons from  $\pi^0$ -decay and electrons from  $\pi^{\pm} \to \mu^{\pm} \to e^{\pm}$ -decay turn out to be relatively featureless,  $\mu^{\pm}$  and p synchrotron radiation and their cascade radiation produce a double-humped spectral energy distribution. For the present model we find p synchrotron radiation to dominate the TeV emission, while the contribution from the synchrotron radiation of the pairs, produced by the high energy hump, is only minor.

## I THE CO-ACCELERATION SCENARIO

With its giant outburst in 1997, emitting photons up to 24 TeV and 0.5 MeV in the  $\gamma$ -ray and X-ray bands, Mkn 501 has proved to be the most extreme TeV-blazar observed so far (e.g. Catanese et al 1997, Pian et al 1997, Aharonian et al 1999).

In this paper, we consider the April 1997 flare of Mkn 501 in the light of a modified version of the Synchrotron Proton Blazar model (SPB) (Mannheim 1993), and present a preliminary model fit.

In the model, shock accelerated protons (p) interact in the synchrotron photon field generated by the electrons  $(e^-)$  co-accelerated at the same shock. This scenario may put constraints on the maximum achievable particle energies.

The usual process considered for accelerating charged particles in the plasma jet is diffusive shock acceleration (see e.g. Drury 1983, Biermann & Strittmatter 1987). If the particle spectra are cut off due to synchrotron losses, the ratio of the maximum particle energies  $\gamma_{p,max}/\gamma_{e,max}$  can be derived by equating  $t_{acc,p}/t_{acc,e} = t_{syn,p}/t_{syn,e}$ , with  $t_{syn,p}$  and  $t_{syn,e}$  being the synchrotron loss time scales for p and  $e^-$ , respectively. We find that for shocks of compression ratio 4 (see Mücke & Protheroe 1999 for a detailed derivation)

$$\frac{\gamma_{p,\text{max}}}{\gamma_{e,\text{max}}} \le \frac{m_p}{m_e} \left(\frac{m_p}{m_e}\right)^{\frac{2(\delta-1)}{3-\delta}} \sqrt{\frac{F(\theta,\eta_{e,\text{max}})}{F(\theta,\eta_{p,\text{max}})}} = \frac{m_p}{m_e} \sqrt{\frac{\eta_{e,\text{max}}F(\theta,\eta_{e,\text{max}})}{\eta_{p,\text{max}}F(\theta,\eta_{p,\text{max}})}}$$
(1)

where the "="-sign corresponds to synchrotron loss, and the "<"-sign to adiabatic loss determining the maximum energies.  $\delta$  is the power law index of the magnetic turbulence spectrum ( $\delta = 5/3$ : Kolmogorov turbulence,  $\delta = 3/2$ : Kraichnan turbulence, and  $\delta = 1$  corresponds to Bohm diffusion).  $\eta_{e,\text{max}}$  is the mean free path at maximum energy in units of the particle's gyroradius and  $F(\theta, \eta_{e,\text{max}})$  takes account of the shock angle  $\theta$  (Jokipii 1987). The ratio  $F(\theta, \eta_{e,\text{max}})\eta_{e,\text{max}}/F(\theta, \eta_{p,\text{max}})\eta_{p,\text{max}}$  can be constrained by the variability time scale  $t_{\text{var}}$ , requiring  $t_{\text{var}}D \geq t_{\text{acc},p,\text{max}}$  (D = Doppler factor,  $t_{\text{acc},p,\text{max}}$  = acceleration time scale at maximum particle energy) for a given parameter combination. As an example, we adopt D = 10, B = 20G and  $t_{\text{var}} = 2$  days. Eq. 1 then restricts for these parameters the ratio of the allowed maximum particle energies to the range below the solid lines shown in Fig. 1. Points exactly on this line correspond to synchrotron-loss limited particle spectra which are accelerated with exactly the variability time scale.

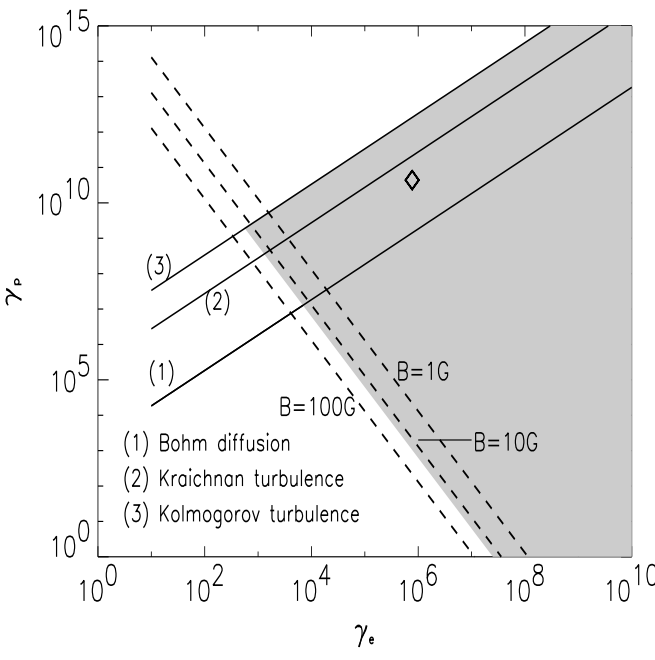


**FIGURE 1.** Allowed parameter space (shaded area) for  $\gamma_{p,\text{max}}$ ,  $\gamma_{e,\text{max}}$  in the SBP-model for typical TeV-blazar parameters (B=20 G, D=10,  $u_1 = 0.5c$ ,  $\beta = 1$ ,  $t_{\text{var}} = 2\text{days}$ ) and for different magnetic turbulence spetra  $I(k) \propto k^{-\delta}$ . The diamond symbol corresponds to the Mkn 501-model presented below.

In hadronic models  $\pi$  photoproduction is essential for  $\gamma$ -ray production. The threshold of this process is given by  $\epsilon_{\rm max}\gamma_{p,{\rm max}}=0.0745$  GeV where  $\epsilon_{\rm max}$  is the maximum photon energy of the synchrotron target field. Inserting  $\epsilon_{\rm max}=3/8\gamma_{e,{\rm max}}^2B/(4.414\times 10^{13}{\rm G})~{\rm m_ec^2}$  into the threshold condition, we find

$$\gamma_{p,\text{max}} \ge 1.72 \cdot 10^{16} (\frac{B}{\text{Gauss}})^{-1} \gamma_{e,\text{max}}^{-2}$$

which is shown in Fig. 1 as dashed line for various magnetic field strengths. Together with Eq. 1, the allowed range of maximum particle energies is then restricted to the shaded area in Fig. 1.

## II THE MKN 501 FLARE IN THE SYNCHROTRON PROTON BLAZAR (SPB) MODEL

We assume the parameters used in Fig. 1, and that the co-accelerated  $e^-$  produce the <u>observed</u> synchrotron spectrum, unlike in previous SPB models, and this is the target radiation field for the  $p\gamma$ -interactions. This synchrotron spectrum, and its hardening with rising flux, has recently been convincingly reproduced by a shock model with escape and synchrotron losses (Kirk et al 1998). We use the Monte-Carlo technique for particle production/cascade development, which allows us to use exact cross sections.

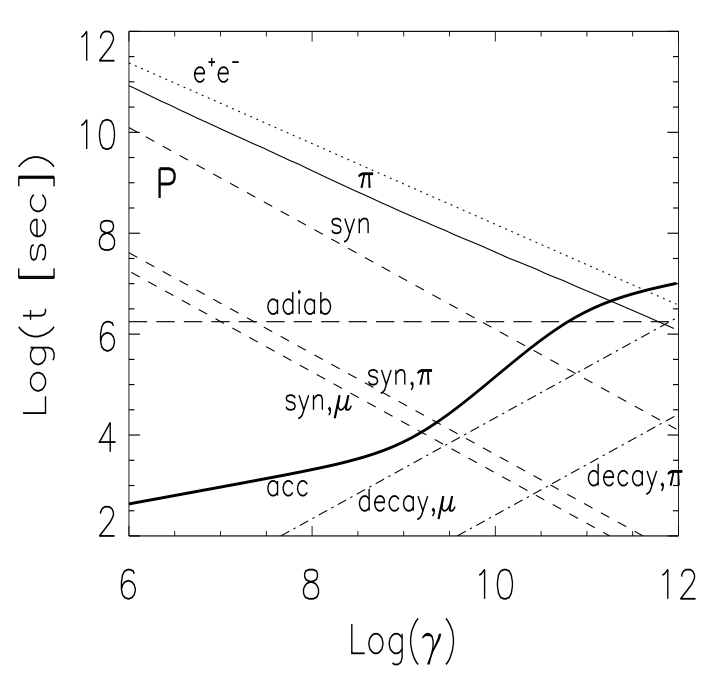


FIGURE 2. Mean energy loss time of p for synchrotron radiation (syn),  $\pi$ -photoproduction ( $\pi$ ) and Bethe-Heitler pair production  $(e^{\pm})$ , and for  $\pi^{\pm}$ - and  $\mu^{\pm}$ -synchrotron radiation (syn  $\pi$ , syn  $\mu$ ) for B = 19.6 G with their mean decay time scales (decay  $\pi$ , decay  $\mu$ ) in the SPB-model. The acceleration time scale (acc), based on Kolmogorov turbulence, is calculated for  $u_1 = 0.5c$ ,  $\eta_p = 40$  and shock angle  $\theta = 85^{\circ}$ . Its curvature reflects the influence of the shock angle. The adiabatic loss time (adiab) is assumed to be  $R/u_1 \approx Dt_{var}$ . All 12 quantities are in the jet frame.

For simplicity we represent the observed synchrotron spectrum (target photon field for the  $p\gamma$ -collisions) as a broken power law in the jet frame with photon power law index 1.4 below the break energy of 0.2 keV, and index 1.8 up to 50 keV.

The variability time scale restricts the radius R of the emission region. Since this region is optically thick to TeV-photons but thin at X-rays, the respective variability time scales are related through  $t_{\rm var,TeV} \approx t_{\rm var,x}/\tau_{\gamma\gamma,\rm TeV}$  (Rachen, these proceedings) with  $t_{\rm var,x}$  being the relevant time scale. For our model we use  $t_{\rm var,x} \approx 2$  days (Catanese et al 1997), and find  $R \approx 2.6 \times 10^{16} {\rm cm}$  for D = 10, B = 19.6 G.

Our model considers photomeson production (simulated using SOPHIA, Mücke et al 1999), Bethe-Heitler pair production (simulated using the code of Protheroe & Johnson 1996), p synchrotron radiation and adiabatic losses due to jet expansion. The mean energy loss and acceleration time scales are presented in Fig. 2.

Synchrotron losses, which turn out to be at least as important as losses due to  $\pi$  photoproduction for the assumed 2 day variability, limit the injected p spectrum  $\propto \gamma_p^{-2}$  to  $2 \leq \gamma_p \leq 4.4 \times 10^{10}$ . This leads to a p energy density  $u_p \approx 0.2 \text{ TeV/cm}^3$ ,

which is bracketed by the photon energy density  $u_{\text{target}} \approx 0.01 \text{ TeV/cm}^3$ , and a magnetic field energy density  $u_B \approx 9.5 \text{ TeV/cm}^3$ . With  $u_B \gg u_{\text{target}}$  significant Inverse Compton radiation from the co-accelerated  $e^-$  is not expected.

Rachen & Meszaros (1998) noted the importance of synchrotron losses of  $\mu^{\pm}$ -(and  $\pi^{\pm}$ -) prior to their decay in AGN jets and GRBs. For the present model, the critical Lorentz factors  $\gamma_{\mu} \approx 3 \times 10^{9}$  and  $\gamma_{\pi} \approx 4 \times 10^{10}$ , above which synchrotron losses dominate above decay, lie well below the maximum particle energy for  $\mu^{\pm}$ , while  $\pi^{\pm}$ -synchrotron losses can be neglected due to the shorter decay time.

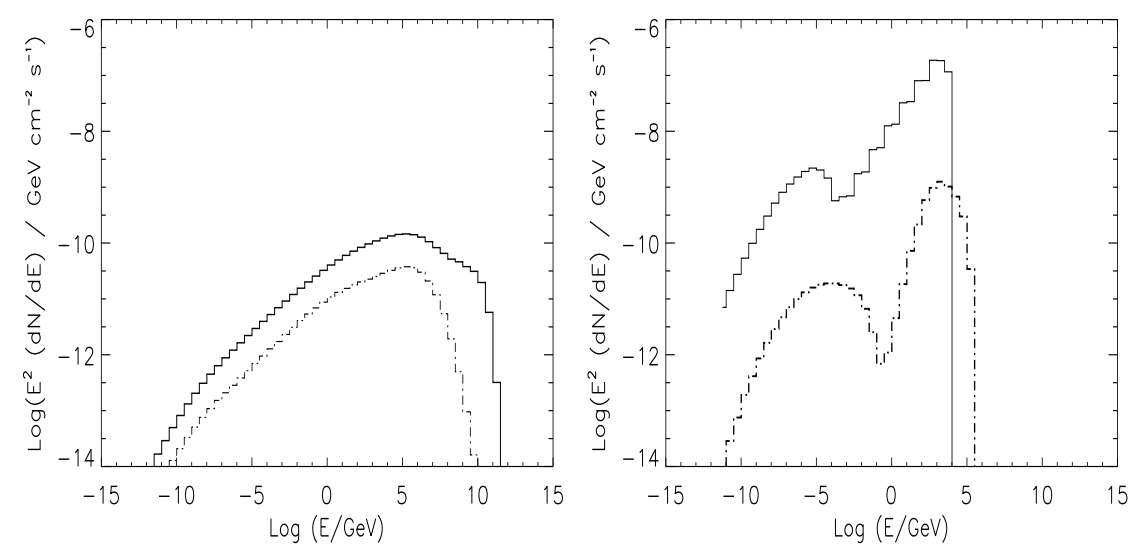


**FIGURE 3.** Left: Average emerging cascade spectra initiated by  $\pi^0$ -decay (solid line) and  $\pi^{\pm}$ -decay synchrotron photons (dashed-dotted line). Right: Average emerging cascade spectra initiated by p- (solid line) and  $\mu^{\pm}$ -synchrotron photons (dashed-dotted line).

The matrix method (e.g. Protheroe & Johnson 1996) is used to follow the pair-synchrotron cascade in the ambient synchrotron radiation field and magnetic field, developing as a result of photon-photon pair production. The cascade can be initiated by photons from  $\pi^0$ -decay (" $\pi^0$ -cascade"), electrons from the  $\pi^{\pm} \to \mu^{\pm} \to e^{\pm}$ -decay (" $\pi^{\pm}$ -cascade"),  $e^{\pm}$  from the proton-photon Bethe-Heitler pair production ("Bethe-Heitler-cascade") and p and p-synchrotron photons ("p-synchrotron cascade" and "p-synchrotron cascade"). In this model, the cascades develop linearly.

Fig. 3 shows an example of cascade spectra initiated by photons of different origin, and for the parameter combination given above.  $\pi^0$ - and  $\pi^\pm$ -cascades obviously produce featureless spectra whereas p- and  $\mu^\pm$ -synchrotron cascades cause the typical double hump shaped SED as observed in  $\gamma$ -ray blazars (see also Rachen, these proceedings). The contribution from Bethe-Heitler cascades turns out to be negligible. Direct p- and  $\mu^\pm$ -synchrotron radiation is responsible for the high energy peak, whereas the low energy hump may be either synchrotron radiation from the directly accelerated  $e^-$  and/or by pairs produced by the "low energy hump".

Adding the four components of the cascade spectrum in Fig. 3 and normalizing

to an ambient, accelerated p density of  $n_{tot,p} = 7 \text{ cm}^{-3}$ , we obtain the SED shown in Fig. 4 where it is compared with the multifrequency observations of the 16 April 1997 flare of Mkn 501.

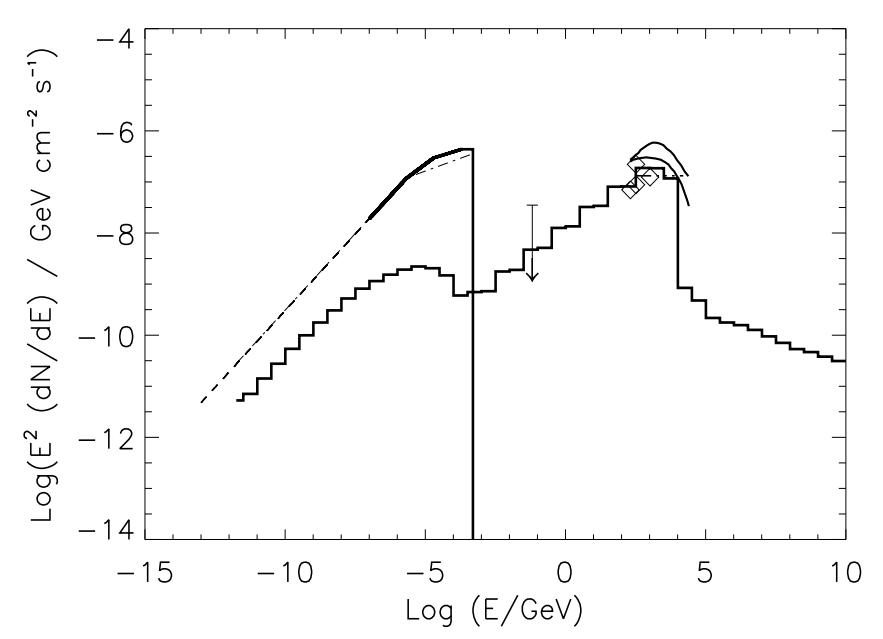


**FIGURE 4.** Present model (histogram) in comparison with the data of the 16 April 1997-flare of Mkn 501. Photon absorption on the cosmic diffuse background radiation field is not included in the model. Straight solid lines: parametrization of the observed, curved synchrotron spectrum (BeppoSAX & OSSE) by Bednarek & Protheroe (1999) and observed TeV-emission corrected for cosmic background absorption (Bednarek & Protheroe 1999) with peak energy output  $\sim 2$  TeV; the 100 MeV upper limit is from Catanese et al 1997 (observed 9-15 April 1997), diamonds: nearly simultaneous (uncorrected) Whipple data (Catanese et al 1997); dashed-dotted line: synchrotron target spectrum.

## REFERENCES

- 1. Aharonian F.A. et al, A&A **342**, 69 (1999).
- 2. Bednarek W. & Protheroe R.J., to appear in MNRAS (1999).
- 3. Biermann, P.L. & Strittmatter, P.A., ApJ 322, 643 (1987).
- 4. Catanese M., et al, ApJ 487, L143 (1997).
- 5. Drury L.O'C, Rep. Prog. Phys. 46, 973 (1983).
- 6. Jokipii J.R., *ApJ* **313**, 842 (1987).
- 7. Kirk J.R., Rieger, F.M. & Mastichiadis, A. A&A 333, 452 (1998).
- 8. Mannheim K.,  $A \mathcal{E} A$  **269**, 67 (1993).
- 9. Mücke A. et al, to appear in Comm. Phys. Comp. (1999).
- 10. Mücke A. & Protheroe R.J., in preparation (1999).
- 11. Pian E. et al, ApJ **492**, L17 (1998).
- 12. Protheroe R.J. & Johnson P., Astropart. Phys. 4 253, & erratum 5, 215 (1996).
- 13. Rachen J.P. & Meszaros P., *Phys.Rev.D* **58**, 123005 (1998).